

Use of Recycled Rubber Granulates in Railway Subballast for Improved Track Performance

Yujie Qi, Ph.D., A.M.ASCE¹; Buddhima Indraratna, Ph.D., F.ASCE.²; and Rakesh Malisetty, Ph.D.³

¹Senior Lecturer and Program Co-leader of Transport Research Centre, School of Civil and Environmental Engineering, University of Technology Sydney, NSW 2007, Australia. ORCID: <https://orcid.org/0000-0002-3486-2130>. Email: yujie.qi@uts.edu.au

²Distinguished Professor of Civil Engineering, Director of Transport Research Centre, School of Civil and Environmental Engineering, University of Technology Sydney, NSW 2007, Australia. ORCID: <https://orcid.org/0000-0002-9057-1514>. Email: buddhima.indraratna@uts.edu.au

³Postdoctoral research fellow, Transport Research Centre, School of Civil and Environmental Engineering, University of Technology Sydney, NSW 2007, Australia. ORCID: <https://orcid.org/0000-0001-8872-2670>. Email: RakeshSai.Malisetty@uts.edu.au

ABSTRACT

As current ballasted tracks are inadequate for supporting Australia's faster, heavier freight trains, there is an urgent need to develop innovative and sustainable alternatives for transport infrastructure. This paper presents a novel solution for increasing the stability and resiliency of railways by developing a sustainable energy-absorbing subballast layer (SEAL) using recycled tire rubber granulates, steel furnace slag, and coal wash to replace traditional rockfill as subballast. The engineering properties of the track incorporating SEAL were investigated through large-scale laboratory tests (i.e. prototype cubic triaxial tests) and a rheological model. The test results and model simulation confirm that the inclusion of recycled rubber granulates actively increases the efficiency of dissipating energy, decreases ballast breakage, vibrations, and the propagation of dynamic loading within the substructure depth. Also, 10% by weight was found to be the optimal rubber content within SEAL to increase the energy-absorbing capacity of the track foundation and decrease the lateral displacements of the track, while reducing the amount of ballast breakage and maintaining an acceptable settlement.

INTRODUCTION

The dynamic loads generated by moving trains exert high energy onto the ballasted-track substructure, leading to progressive degradation over time. These repeated loads cause ballast breakage, particle rearrangement, and permanent deformation, compromising track geometry and stability (Nielsen and Li, 2018). As a result, maintenance requirements increase, operational safety is reduced, and the service life of the infrastructure is shortened. The accumulation of energy within the track system, particularly under high-speed or heavy-haul operations, accelerates wear and damage, making it critical to develop resilient substructure materials and energy-dissipating solutions to enhance track performance and durability under demanding rail traffic conditions (Naeini, et al. 2019).

In response to the above challenge, the use of recycled rubber has gained increasing popularity in railway engineering (Indraratna et al., 2025). Recycled rubber, particularly from end-of-life tires and conveyor belts, offers excellent energy absorption/dissipation and resilience properties,

making it an ideal material for mitigating ballast breakage, vibration, and impact stresses within the ballasted-track substructure (Kelly and Konstantinidis, 2011, Qi et al., 2024). For instance, recycled tire granules were mixed with mining byproducts including coal rejects with or without steel furnace slags, to form a synthetic energy absorbing layer (SEAL) by replacing the conventional subballast/capping layer, which found can efficiently mitigate ballast degradation and load distributed to the soft subgrade (Hidalgo Signes et al., 2015, Hunt et al., 2022, Riyad et al., 2025). Several past studies (e.g. Sol-Sánchez et al., 2015, Koohmishi and Azarhoosh, 2020, Indraratna et al., 2021, Qiang et al., 2023, Indraratna et al., 2024) also mixed recycled rubber granules with ballast to provide a cushioning effect to ballast particles, hence mitigating their abrasion and breakage. Rubber geogrid made from recycled conveyor belts, installed at the interface of ballast and subballast, could significantly improve the shear strength, reduce the lateral movement of the ballast, meanwhile improving the energy absorbing property, and reducing the ballast breakage, which is superior to conventional polymer geogrid (Hettiyahandi et al., 2025). Furthermore, incorporating rubber into rail foundations aligns with sustainability goals by diverting waste from landfills and lowering the environmental footprint of infrastructure projects. As a result, its adoption is growing globally in both research and practice.

However, key uncertainties and research gaps remain regarding recycled rubber utilization, particularly the energy-based mechanism mitigating track damage and methods to quantify energy absorption and dissipation within the track substructure. To address these pending issues, this paper introduces the energy absorbing concept of adding a synthetic energy absorbing layer (SEAL, a composite of recycled crumb rubber, steel furnace slag, and coalwash) in lieu of traditional railway subballast, which is then validated through a large-scale track physical modelling. A rheological model is also proposed to investigate the energy dissipation capacity of the track involving SEAL mixtures.

ENERGY ABSORBING CONCEPT

The substitution of conventional subballast with the SEAL aims to introduce an energy-absorbing cushion within the track system. By improving the energy absorption capacity of the SEAL, the amount of energy transmitted to the underlying ballast and subgrade is reduced, assuming a constant total energy input from loading. This reduction in transmitted energy helps mitigate ballast particle breakage. Figure 1 presents an energy absorption flowchart derived from comprehensive laboratory testing on the SEAL composite. The total energy absorbed by SEAL is partitioned into elastic energy (associated with recoverable deformation) and dissipated energy (attributed to plastic deformation, particle friction, and breakage). As the rubber content in SEAL increases, the total absorbed energy rises (Figure 1a), resulting in greater elastic energy due to enhanced elastic deformation (Figure 1b) and increased dissipated energy (Figure 1c). Notably, the rise in dissipated energy primarily stems from increased plastic deformation (Figure 1d), while friction and breakage decrease with higher rubber content (Figure 1e-f). This energy distribution pattern highlights that the improved energy absorption in SEAL is driven by its deformability from rubber inclusion. To optimise track performance, a carefully balanced rubber content in SEAL is essential to maximise energy absorption, reduce ballast degradation, and improve load distribution, while controlling deformation within acceptable limits. Please note, all the SEAL composites indicated in this paper have been mixed with the optimal ratio of slag:coalwash =7:3 by mass (Qi et al., 2019) to eliminate the swelling potential of steel furnace slag. The rubber content changes between 0-40% within the total mass of the mixture as a further addition of rubber would induce

severe deformation and a bouncing effect (Lee et al. 2014). The small-scale static and cyclic triaxial test results from Indraratna et al. (2025) and Qi et al. (2018) were used to plot Figure 1.

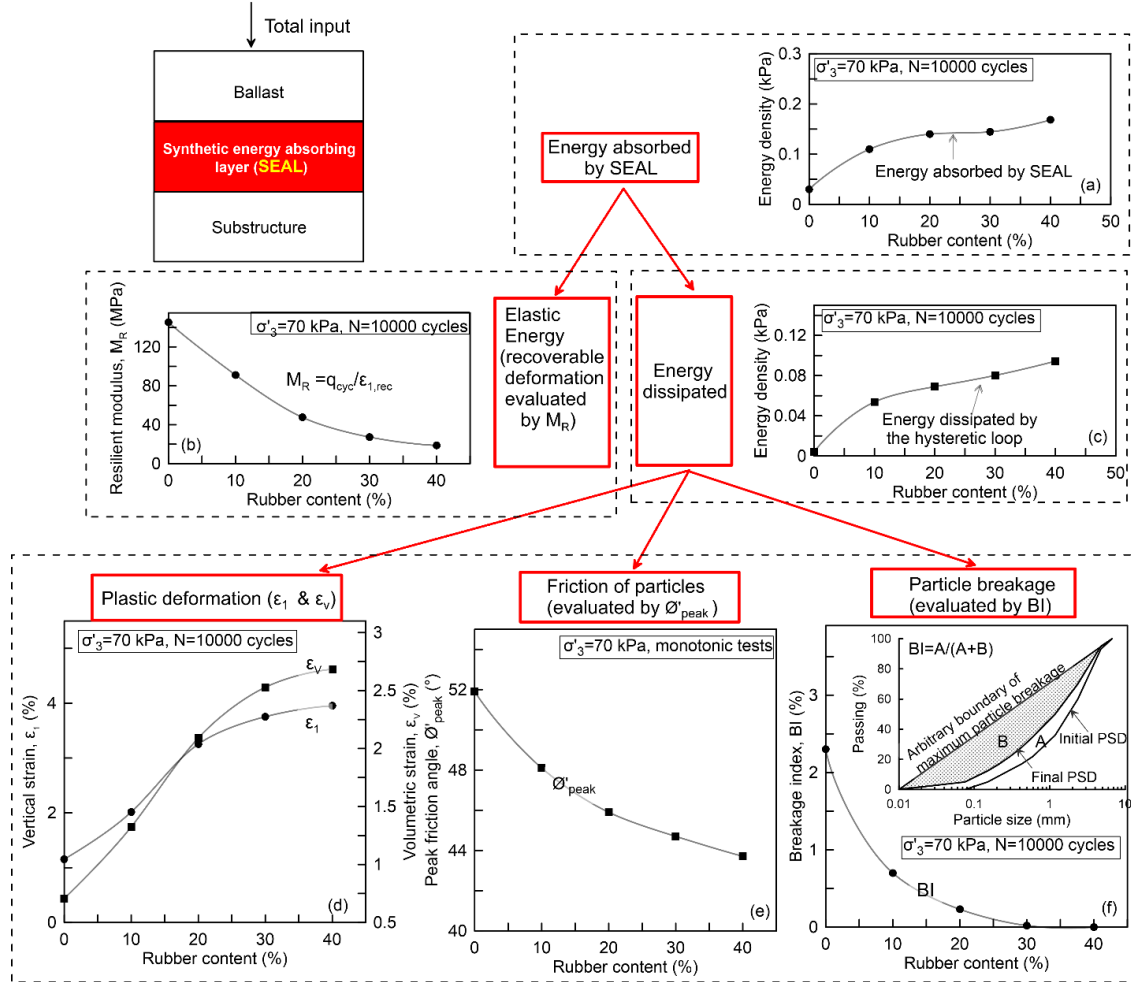


Figure 1. Energy absorbing concept flowchart (modified after Qi et al., 2018)

PHYSICAL MODELING

Large-scale physical modelling using the cubic triaxial apparatus was conducted with the aim of validating the energy-absorbing concept. This enables the investigation of the performance of a unit cell of the track (rail-sleeper-ballast-subballast-subgrade) under cyclic loading. Figure 2a shows the dimensions of the test specimen, where the subballast layer varied with the conventional material (crushed rock) and the SEAL composite (0 - 40% rubber). Each layer of the test specimen was compacted to the field conditions, and the cyclic loading was applied with a frequency = 15 Hz and a maximum axial stress = 230 kPa to mimic a train of 25-ton axle load running at 110 km/h. To simulate a plane strain condition, the side walls of the testing chamber parallel to the sleeper were set still by applying equivalent inverse loading, and the other two side walls were movable (Figure 2b) under a low confining pressure of 15 kPa to examine the lateral displacement. Each test was continued until either 50,000 cycles or failure was reached. After each test, the

ballast particles directly under the sleeper were separated and sieved again to check particle degradation.

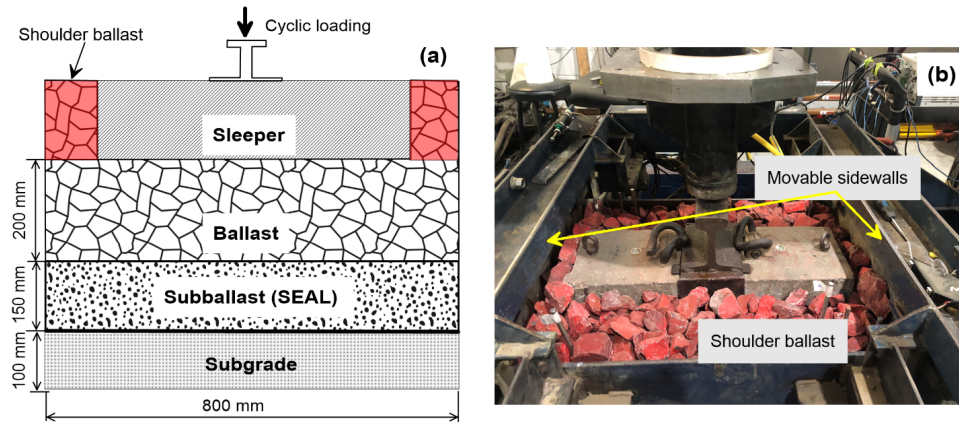


Figure 2. (a) Cross-section view of the physical modeling specimen, (b) a well-prepared test specimen (after Qi and Indraratna et al., 2022a)

Vertical and Lateral Movement

Vertical and lateral displacement of the test specimen are presented in Figure 3. Except for the specimen with SEAL40 (the number after “SEAL” refers to the amount of rubber), which collapsed within 2000 cycles, all the other test specimens were completed successfully to 50,000 cycles and ended with a minimal axial strain rate ($<10^{-8}$), indicating the plastic shakedown was achieved (Malisetty et al., 2022, Qi and Indraratna, 2022b). By increasing the amount of rubber in the SEAL composite, the settlement increases due to the higher compressibility of the SEAL by including rubber. For instance, the settlement is around 8 mm for the specimen with SEAL without rubber, then increases to around 12 mm by adding 10% rubber in SEAL, then jumps to 22 mm when using SEAL30, and then ends with more than 40 mm for SEAL40 after only less than 2000 cycles. Only the test specimens with SEAL0 and SEAL10 exhibit comparable settlement compared to traditional track specimens, ranging between 5 - 14 mm tested by various studies under the same loading conditions. The lateral displacement (dilation in the transverse direction of the track) indicates that the addition of 10 - 20% rubber in SEAL reduces the lateral movement. However, a higher amount of rubber in SEAL (20 - 40%) induces unstable lateral movement as shown in Figure 3b. Compared to conventional test specimens, having SEAL10 shows a 30 - 45% reduction in the lateral dilation. This highlights the benefits of adding SEAL with a proper amount (10%), which can efficiently mitigate the lateral dilation, hence the chances of track buckling.

Damping Ratio and Ballast Degradation

The efficiency of energy dissipation can be evaluated by the damping ratio that can be calculated from the hysteresis loop (Figure 4a), while the ballast breakage can be evaluated via the ballast breakage index (BBI; Indraratna et al., 2005) as defined in Figure (4b). Without rubber in SEAL, there is no improvement in damping, and the BBI is a bit higher compared to traditional materials. By increasing the amount of rubber to 10%, a pronounced rise in damping (by 67%) is noticed, and then the damping gradually increases with the rubber content, indicating that the efficiency of energy dissipation is improved. Accountably, a significant drop in BBI is observed

by using SEAL10 (by 58%). After that, the change in BBI is marginal with the inclusion of rubber in SEAL. This indicates that the improvement in damping may not be fully reflected via the BBI, as energy can be consumed by deformation, particle rearrangement, and friction, apart from breakage. The results of the damping ratio and BBI suggest 10% rubber is preferable, given that with SEAL10, the test specimen exhibits sufficient improvement in damping and reduction in ballast breakage.

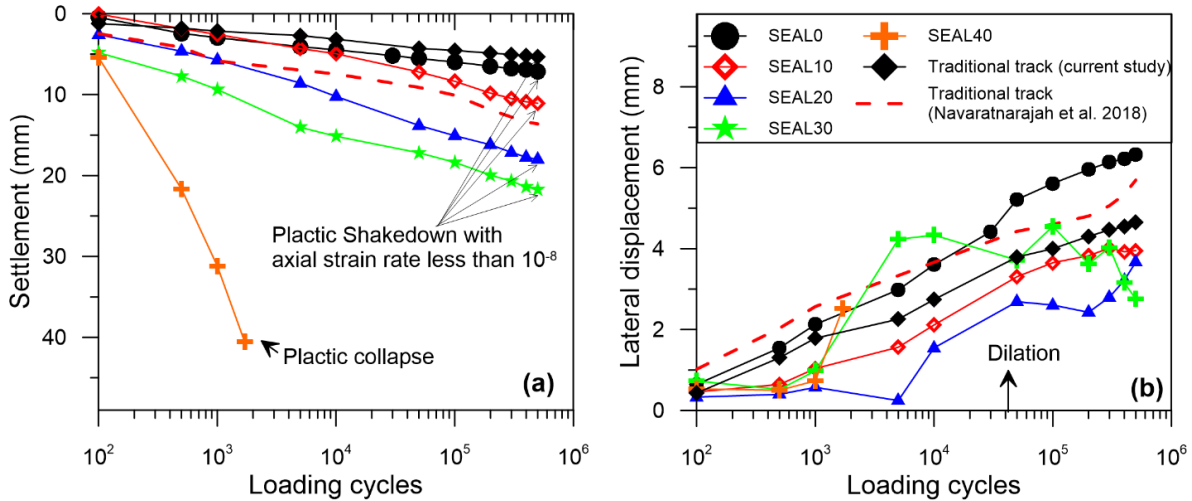


Figure 3. (a) Settlement and (b) lateral movement of test specimens with or without SEAL (modified after Qi and Indraratna, 2022a)

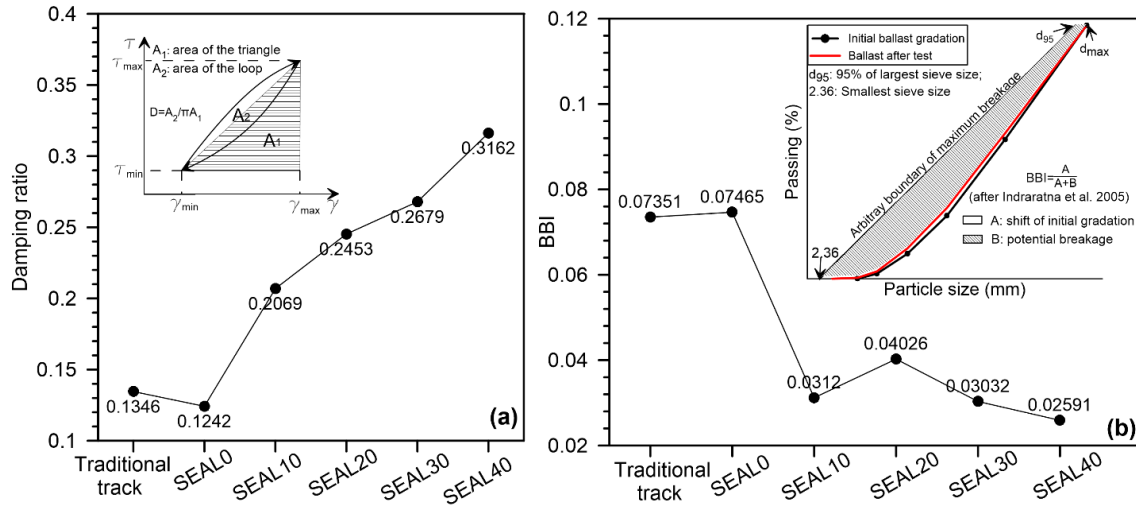


Figure 4. (a) Damping ratio and (b) BBI of test specimens with or without SEAL

SUBSTRUCTURE RHEOLOGICAL MODEL

Considering the enhanced energy absorption of SEAL as discussed in previous sections, it is pertinent to understand how it will help in dissipating excess energy generated by impact loads imparted by wheel-rail contact imperfections. For this, a rheological model to analyse the vibrational characteristics of track substructure with and without SEAL is developed as shown in

Figure 5a. The relevant material properties of SEAL were obtained from the physical modelling. Discrete elements are used to represent ballast, capping, and subgrade layers and are connected by spring-dashpots representing stiffness and damping of each layer. For each substructure element, mass, stiffness, and damping coefficient are determined by considering a pyramidal distribution of vertical load imparted at the sleeper-ballast interface to the substructure layers (Ahlbeck et al., 1978, Punetha et al., 2020). A schematic of load distribution pyramids in the track substructure layers are shown in Figure 5b.

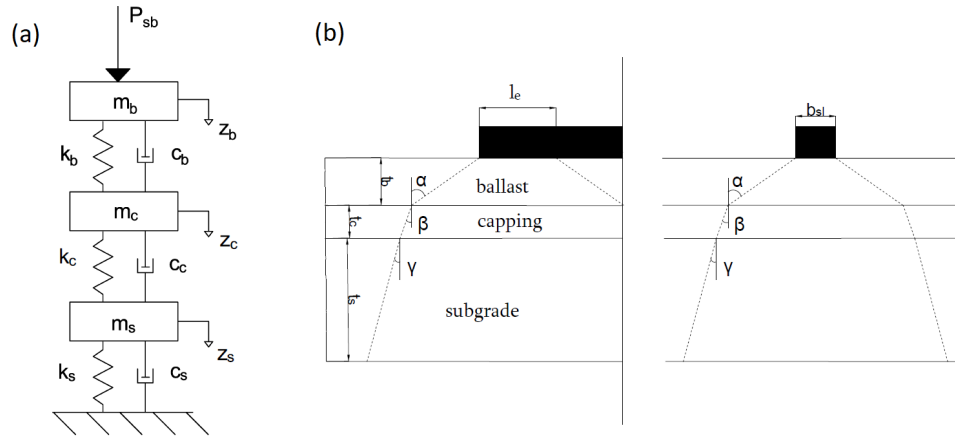


Figure 5. (a) Rheological model of ballasted track substructure (b) Effective substructure regions under the sleeper

The mass (m) and stiffness (k) of each layer are calculated based on the effective regions within the pyramids, which are as follows:

$$M_b = \rho_b t_b \left\{ l_e b_{sl} + (l_e + b_{sl}) t_b \tan \alpha + \frac{4}{3} t_b^2 \tan^2 \alpha \right\} \quad (1)$$

$$m_c = \rho_c t_c \left\{ l_e b_{sl} + (l_e + b_{sl}) (2t_b \tan \alpha + t_c \tan \beta) + 4t_b \tan \alpha (t_b \tan \alpha + t_c \tan \beta) + \frac{4}{3} t_c^2 \tan^2 \beta \right\} \quad (2)$$

$$m_s = \rho_s t_s \left\{ l_e b_{sl} + (l_e + b_{sl}) (2t_b \tan \alpha + 2t_c \tan \beta + h_s \tan \gamma) + 4(2t_b \tan \alpha + t_c \tan \beta) (t_b \tan \alpha + t_c \tan \beta + t_c \tan \gamma) + \frac{4}{3} t_s^2 \tan^2 \gamma \right\} \quad (3)$$

$$k_b = \frac{2(l_e - b_{sl}) \tan \alpha}{\ln \left(\frac{l_e}{b_{sl}} \frac{b_{sl} + 2t_b \tan \alpha}{l_e + 2t_b \tan \alpha} \right)} E_b \quad (4)$$

$$k_c = \frac{2(l_e - b_{sl}) \tan \beta}{\ln \left(\frac{l_e + 2t_b \tan \alpha}{b_{sl} + 2t_b \tan \alpha} \frac{b_{sl} + 2t_b \tan \alpha + 2t_c \tan \beta}{l_e + 2t_b \tan \alpha + 2t_c \tan \beta} \right)} E_c \quad (5)$$

$$k_s = \frac{2(l_e - b_{sl}) \tan \gamma}{\ln \left(\frac{l_e + 2t_b \tan \alpha + 2t_c \tan \beta}{b_{sl} + 2t_b \tan \alpha + 2t_c \tan \beta} \frac{b_{sl} + 2t_b \tan \alpha + 2t_c \tan \beta + 2t_s \tan \gamma}{l_e + 2t_b \tan \alpha + 2t_c \tan \beta + 2t_s \tan \gamma} \right)} E_s \quad (6)$$

In Eqs. (1-6), suffix b, c, s and sl represent ballast, capping, subgrade, and sleeper, respectively. E, t and ρ are the elastic modulus, thickness, and density, and l_e and b_{sl} are the effective length and width of the sleeper, respectively. In this study, it is considered that the $l_e =$ one-third of the length of the sleeper. α, β and γ are the angles of pyramidal stress distribution with depth in ballast, capping, and subgrade layers, respectively, which are determined based on Burmister's theory of stress distribution in layered soil (Burmister, 1958). Considering the mass and stiffness for each layer in Eqs. 1-6, the equations of motion for the track substructure system under the incident sleeper-ballast interface load P_{sb} can be written in a simplified form as:

$$\begin{bmatrix} m_b & 0 & 0 \\ 0 & m_c & 0 \\ 0 & 0 & m_s \end{bmatrix} \begin{bmatrix} \dot{z}_b \\ \dot{z}_c \\ \dot{z}_s \end{bmatrix} + \begin{bmatrix} C_b & -C_b & 0 \\ -C_b & C_b + C_c & -C_c \\ 0 & -C_c & C_c + C_s \end{bmatrix} \begin{bmatrix} z_b \\ z_c \\ z_s \end{bmatrix} + \begin{bmatrix} k_b & -k_b & 0 \\ -k_b & k_b + k_c & -k_c \\ 0 & -k_c & k_c + k_s \end{bmatrix} \begin{bmatrix} z_b \\ z_c \\ z_s \end{bmatrix} = \begin{bmatrix} P_{sb} \\ 0 \\ 0 \end{bmatrix} \quad (7)$$

where, C denotes the damping coefficient, which is determined by taking the product of the damping ratio (ζ) and the critical damping coefficient ($C_{cr} = 2\sqrt{km}$). In the above equation, z represents the vertical movement of each substructure element with positive (+) in the downward direction, and $P_{sb} = l_e b_{sl} \sigma_{sb}$, with σ_{sb} being the vertical stress recorded at the sleeper-ballast interface. The material parameters considered for analysis in this study are given in Table 1. The parameters of the capping layer are interchanged between conventional subballast materials and SEAL materials with different compositions of SFS (steel furnace slag), CW (coalwash), and RC (rubber crumbs), for which the properties are estimated based on experimental investigations (Qi and Indraratna, 2022a).

Table 1. Material parameters

Parameter \ Layer	Ballast	Capping		Subgrade
		Traditional capping	SEAL10	
Thickness (m)	0.3	0.15	0.15	0.5
Elastic modulus (MPa)	200	140	65	150
unit weight (kN/m ³)	15.3	21	17	16
damping ratio (%)	4	9	21	2

The energy dissipation mechanism of SEAL is investigated using the ratio of energy dissipated (E_d) by capping to that by ballast, where E_d is given by:

$$E_d = \int_0^t \dot{z}^T C \dot{z} dt \quad (8)$$

For the analysis, a dynamic stress of 430 kPa measured at the sleeper-ballast interface by Indraratna et al. (2010) at Bulli (NSW, Australia) caused by a wheel flat is considered for a duration of 5 milliseconds. Figure 6 (a-b) shows the attenuation of vertical accelerations with time generated in the ballast layer by the loading impulse and the corresponding power spectrum compared for 150mm-thick traditional subballast, 150 mm and 200 mm-thick SEAL with 10% rubber crumbs. High accelerations are generated at the time of impact which are then attenuated with time. It can be observed that the magnitude of accelerations is lower for SEAL10 when

compared to traditional subballast. Looking at the frequency spectrum of accelerations (Figure 6b), it can be concluded that SEAL10 is able to reduce the magnitude at the two lowest natural frequencies by more than 40%. Also, it is found that the effectiveness of SEAL10 can be increased by increasing its thickness to 200 mm. Similarly, when the energy dissipated by different layers is compared, it can be clearly seen that the energy dissipated by ballast is reduced from 38% to 11% and 7.42% when SEAL10 of 150 mm and 200 mm are used instead of traditional subballast (Figure 7). This can be attributed to the higher damping of SEAL10, enhancing its energy absorption capacity and thus protecting ballast from breakage. Furthermore, it can be observed that the fraction of energy absorbed by the subgrade also reduces with the introduction of SEAL10, which further demonstrates its ability to absorb and mitigate energy propagation to the weaker subgrade layers.

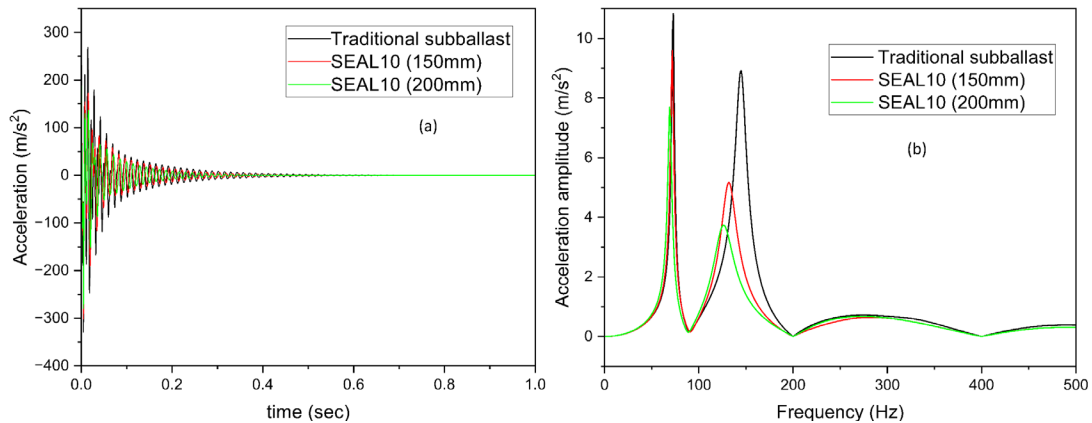


Figure 6. (a) Time series and (b) frequency series of accelerations in the ballast layer with and without SEAL

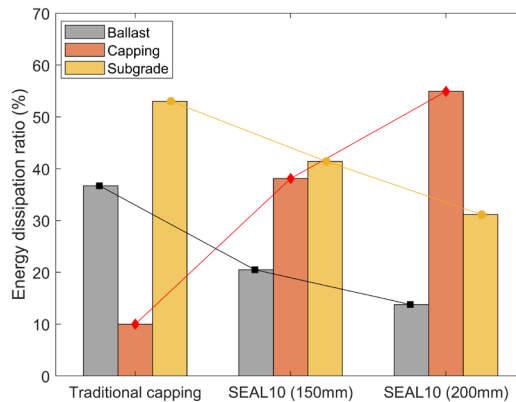


Figure 7. Energy dissipation ratio of different substructure layers

CONCLUSION

This paper investigated the performance of ballasted track incorporated with a synthetic energy-absorbing layer (SEAL) from an energy perspective. An energy consumption flowchart was first introduced, which indicated that the percentage of rubber in SEAL needs to be optimized to balance the energy for particle breakage and deformation. The large-scale physical model was

conducted to validate the energy-absorbing concept for the SEAL-incorporated track. It showed that more rubber in the SEAL led to more deformation and higher damping for a unit-track sample. Also, the test results suggested that 10% rubber was the optimal content, given that it would efficiently reduce the ballast breakage (by 58%), increase the damping property (by 67%), and maintain a comparable settlement compared with conventional track materials. A rheological model was further developed and confirmed that SEAL10 was the optimal by significantly reducing the acceleration (natural frequency) by 40% compared to conventional track materials, and by increasing the SEAL layer from 150 mm to 200 mm thick, the energy went to other layers (ballast and subgrade) could also be reduced further. These research outcomes highlight the ability of SEAL with 10% rubber to efficiently absorb and distribute the energy to enhance track performance with mitigated ballast deterioration and track lateral dilation. Future research should address limitations of this research, including the effects of rubber size and shape and deformation control during field construction.

ACKNOWLEDGMENTS

The authors would like to acknowledge the financial support from the Australian Research Council for ARCLP200200915 and ARCDP220102862. The authors would also like to express appreciation for the technical and financial support from industry partners, including Sydney Trains, SMEC Australia Pty. Limited, and Bestech Australia Pty. Limited.

REFERENCES

- Ahlbeck, D., Meacham, H. and Prause, R. 1978. The development of analytical models for railroad track dynamics. *Railroad track mechanics and technology*, Elsevier: 239-263.
- Burmister, D. M. 1958. "Evaluation of pavement systems of the WASHO road test by layered system methods." *Highway Research Board Bulletin*(177).
- Hettiyahandi, S., Indraratna, B., Ngo, T., Qi, Y. and Arachchige, C. 2025. "Enhancing Rail Track Performance Using Recycled Rubber Energy-Absorbing Grids: Laboratory and Field Evidence." *Journal of Geotechnical and Geoenvironmental Engineering* 151(7): 04025060.
- Hidalgo Signes, C., Martínez Fernández, P., Medel Perallón, E. and Insa Franco, R. 2015. "Characterisation of an unbound granular mixture with waste tyre rubber for subballast layers." *Materials and Structures* 48: 3847-3861.
- Hunt, H., Indraratna, B. and Qi, Y. 2022. "Ductility and energy absorbing behaviour of coal wash-rubber crumb mixtures." *International Journal of Rail Transportation* 11(4): 508-528.
- Indraratna, B., Arachchige, C. M., Rujikiatkamjorn, C., Qi, Y. and Heitor, A. 2024. "Utilization of Granular Wastes in Transportation Infrastructure." *Geotechnical Testing Journal* 47(1): GTJ20220233.
- Indraratna, B., Lackenby, J. and Christie, D. 2005. "Effect of confining pressure on the degradation of ballast under cyclic loading." *Géotechnique* 55(4): 325-328.
- Indraratna, B., Nimbalkar, S., Christie, D., Rujikiatkamjorn, C. and Vinod, J. 2010. "Field assessment of the performance of a ballasted rail track with and without geosynthetics." *Journal of geotechnical and geoenvironmental engineering* 136(7): 907-917.
- Indraratna, B., Qi, Y., Jayasuriya, C., Rujikiatkamjorn, C. and Arachchige, C. M. 2021. "Use of Recycled Rubber Inclusions with Granular Waste for Enhanced Track Performance." *Transportation Engineering*: 100093.

- Indraratna, B., Qi, Y. and Rujikiatkamjorn, C. 2025. *Waste Materials Utilisation for Transport Infrastructure*, CRC Press.
- Kelly, J.M. and Konstantinidis, D., 2011. *Mechanics of rubber bearings for seismic and vibration isolation*. John Wiley & Sons.
- Koohmishi, M. and Azarhoosh, A., 2020. "Hydraulic conductivity of fresh railway ballast mixed with crumb rubber considering size and percentage of crumb rubber as well as aggregate gradation". *Construction and Building Materials*, 241, p.118133.
- Lee, C., Shin, H. and Lee, J.S., 2014. "Behavior of sand–rubber particle mixtures: experimental observations and numerical simulations". *International Journal for Numerical and Analytical Methods in Geomechanics*, 38(16), pp.1651-1663.
- Malisetty, R., Indraratna, B., Qi, Y. and Rujikiatkamjorn, C. 2022. "Shakedown response of recycled rubber-granular waste mixtures under cyclic loading." *Géotechnique* 73(10): 843-848.
- Naeini, M., Mohammadinia, A., Arulrajah, A., Horpibulsuk, S. and Leong, M., 2019. "Stiffness and strength characteristics of demolition waste, glass and plastics in railway capping layers". *Soils and Foundations*, 59(6), pp.2238-2253.
- Nielsen, J.C. and Li, X., 2018. "Railway track geometry degradation due to differential settlement of ballast/subgrade–Numerical prediction by an iterative procedure". *Journal of Sound and Vibration*, 412, pp.441-456.
- Punetha, P., Nimbalkar, S. and Khabbaz, H. 2020. "Analytical Evaluation of Ballasted Track Substructure Response under Repeated Train Loads." *International Journal of Geomechanics* 20(7): 04020093.
- Qi, Y. and Indraratna, B. 2022a. "Influence of Rubber Inclusion on the Dynamic Response of Rail Track." *Journal of Materials in Civil Engineering* 34(2): 04021432.
- Qi, Y. and Indraratna, B. 2022b. "The Effect of Adding Rubber Crumbs on the Cyclic Permanent Deformation of Waste Mixtures Containing Coal Wash and Steel Furnace Slag." *Géotechnique* 73(11): 951-960.
- Qi, Y., Indraratna, B., Heitor, A. and Vinod, J. S. 2018. "Effect of rubber crumbs on the cyclic behavior of steel furnace slag and coal wash mixtures." *Journal of Geotechnical and Geoenvironmental Engineering* 144(2): 04017107.
- Qi, Y., Indraratna, B., Heitor, A. and Vinod, J. S. 2019. "Closure to “Effect of Rubber Crumbs on the Cyclic Behavior of Steel Furnace Slag and Coal Wash Mixtures” by Yujie Qi, Buddhima Indraratna, Ana Heitor, and Jayan S. Vinod." *Journal of Geotechnical and Geoenvironmental Engineering* 145(1): 07018035.
- Qi, Y., Indraratna, B., Ngo, T., Arachchige, C. M. and Hettiyahandi, S. 2024. "Sustainable solutions for railway using recycled rubber." *Transportation Geotechnics*: 101256.
- Qiang, W., Jing, G., Connolly, D. P. and Aela, P. 2023. "The use of recycled rubber in ballasted railway tracks: A review." *Journal of Cleaner Production*: 138339.
- Riyad, A., Indraratna, B., Arachchige, C. K., Qi, Y. and Khabbaz, H. 2025. "An Extended Perspective on the Disturbed State Concept for Rubber–Mixed Waste Material Considering Modulus Degradation under Cyclic Loading." *International Journal of Geomechanics* 25(5): 06025002.
- Sol-Sánchez, M., Thom, N., Moreno-Navarro, F., Rubio-Gamez, M. and Airey, G. 2015. "A study into the use of crumb rubber in railway ballast." *Construction and Building Materials* 75: 19-24.